Observation of Individual Microtubule Motor Steps in Living Cells with Endocytosed Quantum Dots

Xiaolin Nan, Peter A. Sims, Peng Chen,[†] and X. Sunney Xie*

Department of Chemistry and Chemical Biology, Harvard University, Cambridge, Massachusetts 02138

Received: November 3, 2005; In Final Form: November 11, 2005

We report the observation of individual steps taken by motor proteins in living cells by following movements of endocytic vesicles that contain quantum dots (QDs) with a fast camera. The brightness and photostability of quantum dots allow us to record motor displacement traces with 300 μs time resolution and 1.5 nm spatial precision. We observed individual 8 nm steps in active transport toward both the microtubule plus- and minus-ends, the directions of kinesin and dynein movements, respectively. In addition, we clearly resolved abrupt 16 nm steps in the plus-end direction and often consecutive 16 nm and occasional 24 nm steps in minus-end directed movements. This work demonstrates the ability of the QD assay to probe the operation of motor proteins at the molecular level in living cells under physiological conditions.

Introduction

Molecular motors are enzymes that convert the chemical energy of ATP into mechanical work, an essential process for life.[1] Kinesin and dynein are two types of motor enzymes that actively transport organelles along microtubules in the cytoplasm. Microtubules have a polar structure with the minus-end near the nucleus of the cell and the plus-end near the membrane. In vitro experiments have shown that kinesin travels toward the microtubule plus-end whereas dynein travels toward the minus-end.[1] The mechanism of chemomechanical coupling has been the subject of intense investigation in vitro.[2−5] These experiments have shown that kinesin takes an 8 nm step along a microtubule during each enzymatic turnover.[2−5] This step size matches the periodicity of the microtubule binding sites. A recent study has shown that dynein takes steps that are integer multiples of 8 nm and depend on the force applied to its cargo.[6]

The next challenge is to understand how the motors work in living cells. In contrast to the clean, in vitro conditions, molecular motors exhibit much more complicated behavior in a cellular environment. Among these complications are the possible involvement of multiple motors on a single cargo,[7−10] the crowdedness and heterogeneity of the cytoplasm, and the participation of accessory proteins.[11,12] With the exception of a recent study using GFP,[10] however, in vivo studies of molecular motors to date have been unable to resolve individual steps because of limited time and spatial resolution. Just as in the in vitro experiments, the ability to resolve individual steps in vivo is critical to our understanding of how motor proteins carry out their functions.

Quantum dots (QDs) are semiconductor nanocrystals with optical properties superior to those of conventional organic fluorophores.[13,14] The exceptional brightness and photostability of QDs make them an ideal probe for biological imaging.[15,16] QDs have been used to observe individual steps of myosin V in vitro through nanometer precision localization of QDs tethered to single motors,[17] similar to the approach of earlier studies with single fluorophores in which much was learned about the stepping behavior of both myosin V and kinesin.[18−20]

The key idea of these experiments is that the centroid position of a sufficiently bright fluorophore can be determined to within nanometer precision by fitting the intensity profile to a two-dimensional Gaussian function, despite the optical diffraction limit.[18−20] In a recent study, Kural et al. used a heavily GFP-tagged peroxisome as a fluorescent probe of motor-stepping in living cells.[10] The authors resolved 8 nm steps taken by both kinesin and dynein in the processes of *Drosophila* S2 cells at 10 °C with a time resolution of 1.1 ms.

Here, we use QDs, which are easily introduced to the cells via endocytosis, as demonstrated previously,[21,22] and subsequently transported along microtubules in endosomes by motor proteins. The exceptional brightness and photostability of QDs over GFP allow us to record long motor displacement traces with a time resolution as high as 230 μs and single-step spatial resolution in the cytoplasm of living cells at 37 °C. We report the observation of individual 8 nm steps taken by microtubule motors traveling in both the plus- and minus-end directions. More interestingly, we observe 16 nm steps taken by motors traveling toward the plus-end, and we frequently see consecutive 16 nm steps and occasional 24 nm steps taken by motors traveling toward the minus-end. It is known from in vitro experiments that a single kinesin motor travels along microtubules toward the plus-end with 8 nm steps. Since the physical size of a kinesin head does not permit a step size of 16 nm, these steps might result from the collective action of multiple motors on a single cargo, for example, motor proteins taking 8 nm steps in a coupled fashion. Dynein, a more complex protein, is known to travel toward the minus-end. Although our observation of large step sizes in the minus direction could be

* Corresponding author. Email: xie@chemistry.harvard.edu.
† Present Address: Department of Chemistry and Chemical Biology, Cornell University, Ithaca, NY 14853.

Letters

J. Phys. Chem. B, Vol. 109, No. 51, 2005 **24221**

explained by multiple motors acting on a single cargo, a single dynein is structurally capable of taking 16 and 24 nm steps as observed in vitro.[6] Our assay provides new clues about motor protein operation in a cellular environment.

Materials and Methods

We culture human lung cancer (A549) cells in Dubecco's Modified Eagle Medium (DMEM, ATCC) supplemented with 10% FBS at 37 °C and 5% CO_2. Cells are plated on a Bioptech Delta T temperature control dish at least 24 h prior to adding QDs.

We used streptavidin-coated QDs (emission at 655 nm) and a biotinated poly(arginine) peptide (both at 2 μM concentration) from Qdots, Inc., as a Qtracker cell labeling kit. We determined the identity of the peptide (Reagent B) to be (Arg)9-Biotin using mass spectrometry. Before adding to the cell culture medium, we incubate the QDs with the peptide briefly at a 1:1 volume ratio. Then, we add the QDs to the culture medium at a final concentration of 200 pM. After a 1 h incubation period, the cells are washed with fresh culture medium and incubated for another 12 h. Immediately following the first incubation, the majority of the QDs are found on the cell membrane resulting in a large fluorescent background that prohibits high-resolution imaging of QDs inside the cell. However, after the second incubation, we observe aggregates of 5−30 QDs in the cytoplasm, according to the total intensity of the aggregates. These QDs are efficiently excited by a 532 nm laser (Verdi 5, Coherent), and they emit at 655 nm, far away from wavelengths of cellular autofluorescence.

We deliver our excitation beam with an optical fiber which is then collimated and delivered to the back of a Nikon TE-300 inverted microscope. To achieve the maximum photon flux and time resolution, we used an excitation scheme in which we positioned a lens (f = 300 mm) to focus the beam onto the back aperture of the objective. This resulted in a collimated excitation beam at the sample and a field of view with a diameter of 25 μm. We collected the fluorescence signal with a 60 × 1.2 NA water-immersion objective (Olympus UPlanApo/IR). A back-illuminated, intensified CCD camera (Cascade 128+, Roper Scientific) was mounted on a 2.5× relay lens to record movies. Typically, we select a region of 12−20 pixel rows (the number of columns does not affect time resolution) on the CCD chip. To achieve 230 μs time resolution, we apply 2 × 2 binning of the pixels. The measured step sizes have no dependence on the frame rates. The acquired frames from the camera were streamed directly to the computer memory, so that we avoid missing frames during data collection.

To clearly resolve the 8 nm steps of kinesin and dynein, we need to suppress both photon and mechanical noise. QD aggregates form diffraction-limited spots on the CCD camera which can be fit to a two-dimensional Gaussian function to determine their centroid positions.[19,20] With our typical excitation power of 20−35 mW (40−70 μW/μm^2 at the sample), we collect as many as 1000 photons per frame at the centroid pixel without binning. Under this condition, the error in the centroid determination is less than 1.5 nm, which we calculated using[18]

$$\sigma \approx \sqrt{\frac{1}{N}\left(s^2 + \frac{a^2}{12}\right)}$$

where N is the number of photons ($\sim$25 000), s is the width of the diffraction-limited spot ($\sim$221 nm), and a is the pixel size (143 nm without binning). At a time resolution of 230−400

μs, QDs are critical to achieving such a high photon flux and spatial precision.

To reduce mechanical noise, we took several extra measures such as building the microscope setup on a floated optical bench, enclosing the optics, and removing all electronic devices other than the camera from the bench. In addition, we replaced the original microscope stage with an Olympus nosepiece stage (IX2-NPS) to eliminate motion of the objective relative to the sample. Another source of noise is the camera fan, which introduces a 75 Hz frequency component to our displacement traces. This is suppressed by mounting the camera on a heavy, metal base. An alternative approach is to use a vacuum hose to eliminate the fan entirely. Mechanical noise is less than 1 nm as measured from the displacement trace of a static bead immobilized on a microscope slide. Overall, the noise intrinsic to our imaging setup is estimated to be less than 2 nm.

We employed a forward−backward nonlinear filter designed by Chung and Kennedy[23] to accurately measure the sizes and dwell times of the steps instead of a low pass filter. The filter is not used to extract steps that are hidden in the raw data but to outline and preserve the edges of steps that are already clearly visible in raw displacement traces.[24] This particular filter uses Baye's Rule to remove Gaussian-distributed noise from the displacement trajectories. If we let $y(k)$ be the experimentally measured displacement trace, then $y(k) = x(k) + n(k)$ where $x(k)$ is the true displacement trace and $n(k)$ is the associated noise. According to this algorithm, the filtered displacement trace, $\hat{x}(k)$ is given by

$$\hat{x}(k) = \sum_{i=1}^{K}[f_i(k)\hat{x}_{f,i}(k) + b_i(k)\hat{x}_{b,i}(k)]$$

where

$$f_i(k) \propto \frac{1}{2K}\left\{\sum_{j=0}^{M-1}[y(k-j) - \hat{x}_{f,i}(k-j)]^2\right\}^{-p}$$

$$b_i(k) \propto \frac{1}{2K}\left\{\sum_{j=0}^{M-1}[y(k+j) - \hat{x}_{b,i}(k+j)]^2\right\}^{-p}$$

are the forward and backward weights (predictors) that are normalized using $\sum_{i=1}^{K}[f_i(k) + b_i(k)] = 1$. M is size of the analysis window, p is a weighting factor that typically ranges between 1 and 100, and K is the number of forward and backward predictors. In our analysis, we typically use $K = 5$, $M = 10$, and $p = 10$. These values fall within the ranges that are recommended by the authors of this algorithm.[23]

Results and Discussion

QDs enter the cells via endocytosis[22] during a 12-h long incubation period, after which they form aggregates in endosomes, and there are essentially no QDs left on the plasma membrane. This incubation effectively reduces the out-of-focus background signal from QDs bound to the basal membrane, and is essential for high contrast imaging with a non-confocal fluorescence microscope. Unlike single QDs in solution, the QD aggregates that are bright enough to be tracked at a time resolution of $\sim$300 μs do not blink,[25] possibly because not all QDs in an aggregate are in a dark state at the same time. The QDs have a cationic coating, which allows them to stick to the membrane and prevents their motion relative to the endosome.
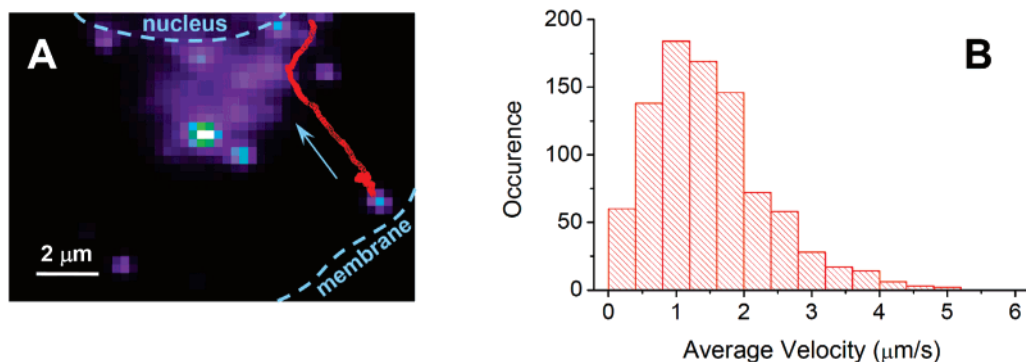
Figure 1. (A) $X-Y$ position trajectory of a vesicle containing a quantum dot aggregate moving from the cell periphery toward the nucleus, in the dynein direction, in a live A549 cell, at an overall average velocity of 1.5 μm/s. (B) Histogram of average velocity along the trajectory shown in (A). The movie was taken with 2.5 ms time resolution, and the velocities are averaged over 12.5 ms.
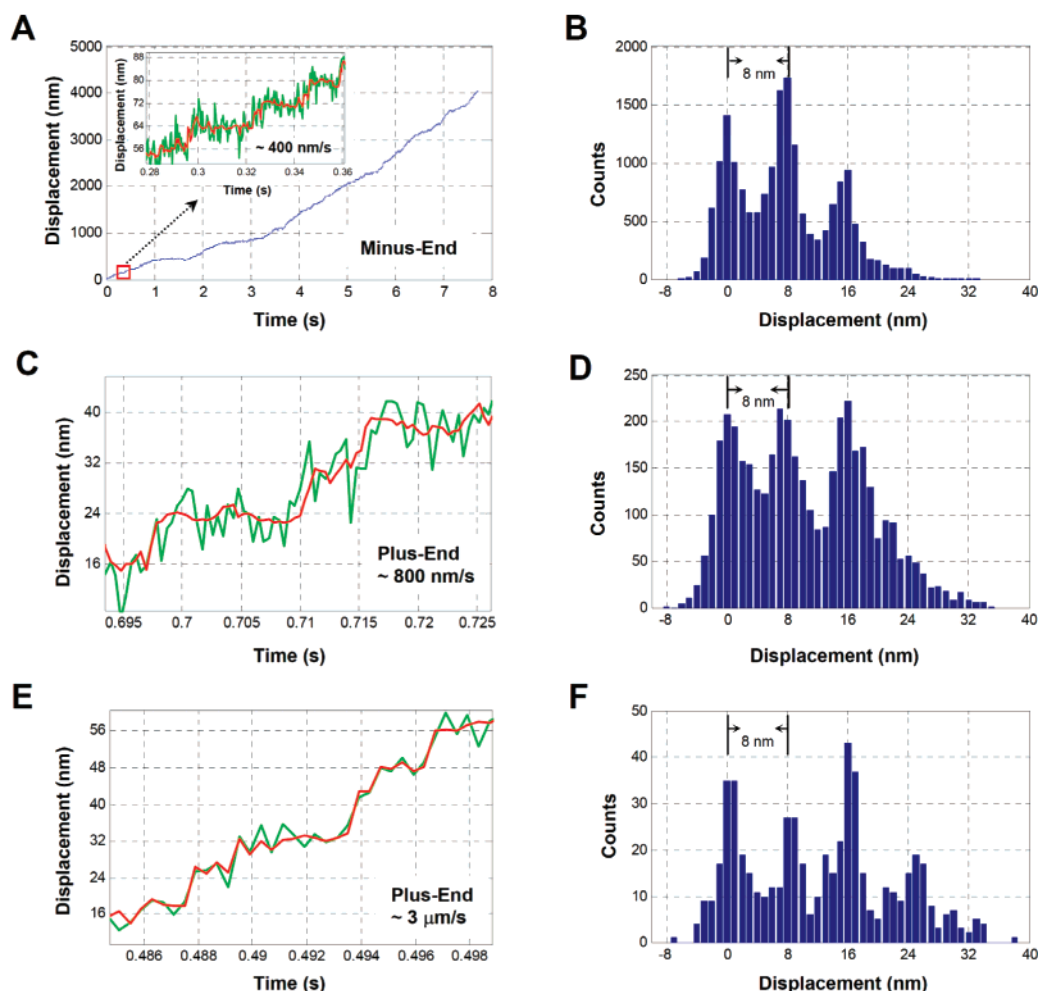
Figure 2. (A) Displacement trace of a vesicle-enclosed QD aggregate being transported toward microtubule minus-end of an A549 cell. The displacement is calculated along the microtubule path, by dividing the original $x-y$ position trajectory into short, straight segments and accumulating the total displacement. Inset: Segment of the displacement trace showing consecutive 8 nm steps at a velocity of 400 nm/s obtained with a time resolution of 370 μs. (B) Pairwise distance histogram for the displacement trace in the inset of (A). (C) Displacement trace segment of a QD aggregate transported toward the microtubule plus-end at a velocity of 800 nm/s obtained with 430 μs time resolution. (D) Corresponding pairwise distance histogram for (C). (E) Displacement trace segment of a plus-end moving QD aggregate at a velocity of 3 μm/s taken with 400 μs time resolution. (F) Corresponding pairwise distance histogram for (E).

Some of the endosomes containing QD aggregates undergo random diffusion, while others bind to motor proteins and undergo active transport. The typical run length of the active transport is a few microns, until the endosome stalls, possibly because of the detachment from microtubules. Figure 1A shows the displacement trace of a QD aggregate that is transported from the cell periphery to the perinuclear region. The velocity of this active transport event ranges from tens of nanometers

per second to 5 μm/s with an average velocity of 1.5 μm/s (Figure 1B), consistent with reported velocities of microtubule motor-mediated active transport.[8] We note that this velocity distribution is markedly different from the recent report[10,26] where the velocity is broadly distributed from 0 to 13 μm/s, possibly because instantaneous speeds associated with short runs (as short as 15 nm) were measured.[27] The active transport is completely abolished when we treat the cells with the micro-
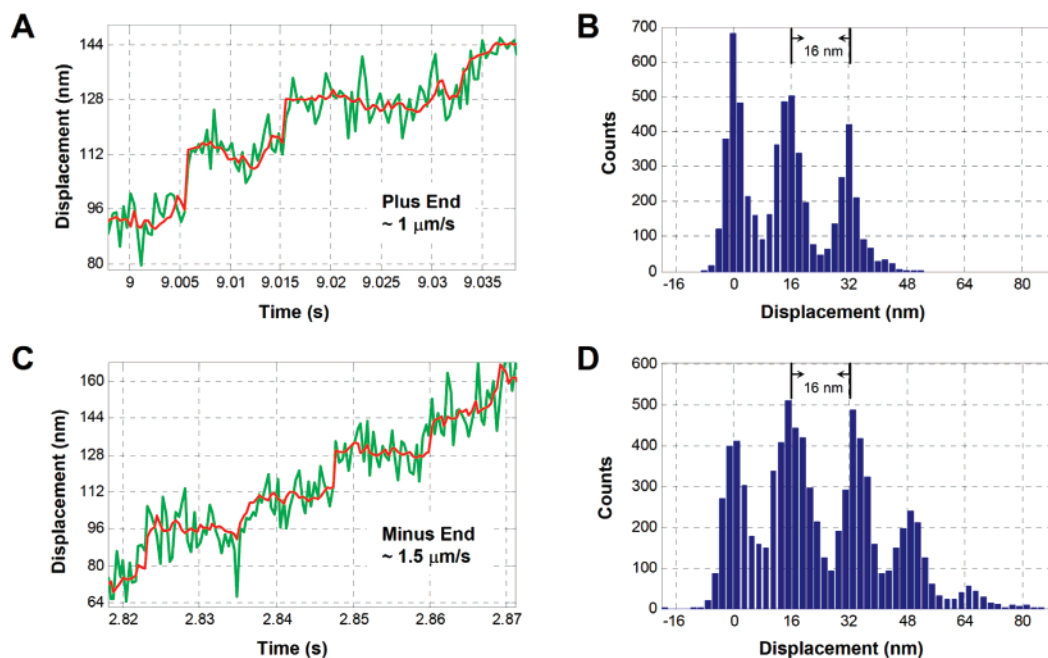
Figure 3. (A) Displacement trace segment of a vesicle-enclosed QD aggregate being transported toward microtubule plus-end of an A549 cell with three consecutive 16 nm steps. The time resolution is 359 μs. (B) Pairwise distance histogram for the displacement trace in (A). (C) Displacement trace segment of a minus-end movement taken with 400 μs time resolution exhibiting consecutive 16 nm steps. (D) Pairwise distance histogram for the displacement trace in (C).

tubule-disruption drug nocodazole, but is unaffected by treatment with the F-actin disruption drug cytochalasin-D. These results indicate that microtubule motors are responsible for the active transport.

It is known that dynein is a microtubule minus-end directed motor, which transports cargos from the cell periphery to the perinuclear region, while kinesin moves in the opposite direction.[8] The directionality of these movements is assigned by viewing the entire cell on a separate CCD camera with a larger field of view. Although there are kinesin variants moving certain organelles toward the microtubule minus-end,[28] endosomes have been shown to undergo active transport mediated by dynein in this direction.[29]

Figure 2A shows a typical displacement trace of an endosome moving toward the microtubule minus-end, the direction of dynein movement. The 8 nm steps are clearly visible in the raw displacement trace (inset, shown in green). Superimposed on the stepwise movements are random motions associated with the confined diffusion of vesicles[30] in the cytoskeletal environment and the movement of microtubules to which the vesicles are attached. The amplitude of these random motions is position-dependent and can be as small as 2−4 nm in some regions of the displacement traces.

However, there are always regions of our displacement traces in which these random motions prevent us from resolving steps. Individual steps can be visualized more clearly after filtering these raw displacement traces with the nonlinear Bayesian filter[23] (Figure 2A, inset, red). The step size is determined with the pairwise distance histogram (Figure 2B), which gives the distribution of distances between any two points along the displacement trace. The step size is given by the periodicity of the pairwise distance histogram.

Similarly, we clearly resolved the 8 nm steps toward the microtubule plus-end, the direction of kinesin movements (Figure 2C,D). Similar 8 nm steps of both kinesin and dynein have been reported by Kural et al. in *Drosophila* S2 cells at 10 °C.[10] We note that our experiment was done at 37 °C. The high time resolution afforded by the QDs and the fast CCD camera

allows us to resolve the individual 8 nm steps taken by endosomes traveling at a velocity as high as 3 μm/s (Figure 2E,F).

Interestingly, in addition to the 8 nm steps, we also observed abrupt 16 nm steps in the plus-end directed movement, sometimes occurring consecutively (Figure 3A,B). Out of the 417 resolved steps in the plus-end displacement traces, 156 (∼37%) are around 16 nm. We cannot distinguish whether such a 16 nm step is an individual physical step or two 8 nm steps very closely spaced in time. It has been well-established by in vitro experiments that single kinesin motors only take 8 nm steps. If a single kinesin is transporting the endosome, we should have sufficient time resolution to resolve the individual 8 nm steps. This is because the k_{cat} of a two-headed kinesin is ∼100 s^{-1},[8] and the probability for a single motor enzyme to produce two consecutive turnovers within 300 μs (our time resolution) is negligible. Since single kinesins are structurally incapable of taking such large steps, one possible explanation is that the observed 16 nm steps are due to the collective activity of more than one motor in transporting the individual cargo. For example, multiple motor proteins might step 8 nm in a coupled fashion. The involvement of multiple motors has been evidenced by previous electron microscopy[7] and optical tweezer experiments.[7,9] Some of our displacement traces (data not shown) exhibit repetitive back-and-forth movements, which could be due to the competetion of multiple motors with opposite directionality ("tug-of-war") or to the entanglement of the cargo in the crowded cytoplasmic environment.

Similarly, in the displacement traces of minus-end directed movements, we also observed abrupt 16 nm steps. Out of the 1107 resolved single steps in the minus direction, 442 (40%) have a step size of ∼16 nm. Unlike in the plus-end displacement traces, these 16 nm steps often occur consecutively (Figure 3C,D), and we even observed occasional 24 nm steps (∼11%). Although the 16 and 24 nm steps could also be attributed to unresolved 8 nm steps of multiple motors, single cytoplasmic dynein motors are structurally capable of taking such big steps.[3] In fact, cytoplasmic dynein has been reported to take 16 and

24 nm steps in vitro.[6] We note that only 8 nm steps were reported for dynein in vivo in the recent study.[10] In comparison with kinesin, the molecular structure[31-34] and biochemistry[35] of dynein are much more complicated. More experiments are clearly required in order to understand the origin of the observed 16 and 24 nm steps.

The observation of large steps of microtubule motors in both directions in live cells, made possible by the QD assay, highlights the complexity of motor operations in vivo and raises new questions regarding the mechanisms of molecular motors.

Conclusion

Much has been learned about motor proteins at the single molecule level through in vitro experiments. Understanding how individual motors work together in a living cell is the next challenge. This requires high time and spatial resolution imaging. We used quantum dots as probes to observe individual steps of dynein and kinesin in living cells. Their brightness and photostability allow us to achieve a time resolution as high as 230 μs and a spatial resolution of 1.5 nm. Quantum dots offer the ability to resolve single motor steps in a broad velocity range under physiological conditions. As expected, we observed 8 nm steps in both minus- and plus-end directed movements. We also observed 16 nm steps in microtubule plus-end directed movements, possibly because of the collective activity of multiple motors on a single cargo. In the minus-end directed movements, large 16 and 24 nm steps were observed. While the involvement of multiple dynein motors is a plausible reason for this observation, the possibility that single dyneins take large steps in vivo as reported in vitro should not be ruled out. Our study highlights the ability of live cell imaging with sub-millisecond temporal and nanometer spatial precision to elucidate the inner workings of macromolecular machineries under physiological conditions.

Note Added after ASAP Publication. This article was published ASAP on December 6, 2005. A change has been made to ref 26. The correct version was published on December 12, 2005.

References and Notes

(1) For reviews, see (a) Schliwa, M.; Woehlke, G. Molecular motors. *Nature (London)* **2003**, *422*, 759−765; (b) Vale, R. D. The molecular toolbox for intracellular transport. *Cell* **2003**, *112*, 467−480 and references therein.

(2) Asbury, C. L.; Fehr, A. N.; Block, S. M. Kinesin moves by an asymmetric hand-over-hand mechanism. *Science* **2003**, *302*, 2130−2134.

(3) Burgess, S. A.; Walker, M. L.; Sakakibara, H.; Knight, P. J.; Oiwa, K. Dynein structure and power stroke. *Nature (London)* **2003**, *421*, 715−718.

(4) Hua, W.; Young, E. C.; Fleming, M. L.; Gelles, J. Coupling of kinesin steps to ATP hydrolysis. *Nature (London)* **1997**, *388*, 390−393.

(5) Schnitzer, M. J.; Visscher, K.; Block, S. M. Force production by single kinesin motors. *Nat. Cell Biol.* **2000**, *2*, 718−723.

(6) Mallik, R.; Carter, B. C.; Lex, S. A.; King, S. J.; Gross, S. P. Cytoplasmic dynein functions as a gear in response to load. *Nature (London)* **2004**, *427*, 649−652.

(7) Ashkin, A.; Schutze, K.; Dziedzic, J. M.; Euteneuer, U.; Schliwa, M. Force generation of organelle transport measured in vivo by an infrared laser trap. *Nature (London)* **1990**, *348*, 346−348.

(8) Howard, J. *Mechanics of Motor Proteins and the Cytoskeleton*; Sinauer Associates, Inc.: Sunderland, Massachusetts, 2001.

(9) Welte, M. A.; Gross, S. P.; Postner, M.; Block, S. M.; Wieschaus, E. F. Developmental regulation of vesicle transport in Drosophila embryos: forces and kinetics. *Cell* **1998**, *92*, 547−557.

(10) Kural, C.; Kim, H.; Syed, S.; Goshima, G.; Gelfand, V. I.; Selvin, P. R. Kinesin and dynein move a peroxisome in vivo: a tug-of-war or coordinated movement? *Science* **2005**, *308*, 1469−1472.

(11) King, S. J.; Schroer, T. A. Dynactin increases the processivity of the cytoplasmic dynein motor. *Nat. Cell Biol.* **2000**, *2*, 20−24.

(12) Gross, S. P. Dynactin: coordinating motors with opposite inclinations. *Curr. Biol.* **2003**, *13*, R320−R322.

(13) Chan, W. C.; Nie, S. Quantum dot bioconjugates for ultrasensitive nonisotopic detection. *Science* **1998**, *281*, 2016−2018.

(14) Bruchez, M., Jr.; Moronne, M.; Gin, P.; Weiss, S.; Alivisatos, A. P. Semiconductor nanocrystals as fluorescent biological labels. *Science* **1998**, *281*, 2013−2016.

(15) Jaiswal, J. K.; Mattoussi, H.; Mauro, J. M.; Simon, S. M. Long-term multiple color imaging of live cells using quantum dot bioconjugates. *Nat. Biotechnol.* **2003**, *21*, 47−51.

(16) Smith, A. M.; Gao, X.; Nie, S. Quantum dot nanocrystals for in vivo molecular and cellular imaging. *Photochem. Photobiol.* **2004**, *80*, 377−385.

(17) Warshaw, D. M.; Kennedy, G. G.; Work, S. S.; Krementsova, E. B.; Beck, S.; Trybus, K. M. Differential labeling of myosin V heads with quantum dots allows direct visualization of hand-over-hand processivity. *Biophys. J.* **2005**, *88*, L30−L32.

(18) Thompson, R. E.; Larson, D. R.; Webb, W. W. Precise nanometer localization analysis for individual fluorescent probes. *Biophys. J.* **2002**, *82*, 2775−2783.

(19) Yildiz, A.; Forkey, J. N.; McKinney, S. A.; Ha, T.; Goldman, Y. E.; Selvin, P. R. Myosin V walks hand-over-hand: single fluorophore imaging with 1.5-nm localization. *Science* **2003**, *300*, 2061−2065.

(20) Yildiz, A.; Tomishige, M.; Vale, R. D.; Selvin, P. R. Kinesin walks hand-over-hand. *Science* **2004**, *303*, 676−678.

(21) Jaiswal, J. K.; Goldman, E. R.; Mattoussi, H.; Simon, S. M. Use of quantum dots for live cell imaging. *Nat. Methods* **2004**, *1*, 73−78.

(22) Osaki, F.; Kanamori, T.; Sando, S.; Sera, T.; Aoyama, Y. A quantum dot conjugated sugar ball and its cellular uptake. On the size effects of endocytosis in the subviral region. *J. Am. Chem. Soc.* **2004**, *126*, 6520−6521.

(23) Chung, S. H.; Kennedy, R. A. Forward−backward nonlinear filtering technique for extracting small biological signals from noise. *J. Neurosci. Methods* **1991**, *40*, 71−86.

(24) Coppin, C. M.; Pierce, D. W.; Hsu, L.; Vale, R. D. The load dependence of kinesin's mechanical cycle. *Proc. Natl. Acad. Sci. USA* **1997**, *94*, 8539−8544.

(25) Hohng, S.; Ha, T. Near-complete suppression of quantum dot blinking in ambient conditions. *J. Am. Chem. Soc.* **2004**, *126*, 1324−1325.

(26) In reference 10, the authors studied peroxisomes moving in the processes of Drosophila "S2" cells at 10 °C, which is a different system from ours.

(27) Kural, C.; Balci, H.; Selvin, P. R. Molecular motors one at a time: FIONA to the rescue. *J. Phys.: Condens. Matter* **2005**, *17*, S3979−S3995.

(28) Noda, Y.; Okada, Y.; Saito, N.; Setou, M.; Xu, Y.; Zhang, Z.; Hirokawa, N. KIFC3, a microtubule minus end-directed motor for the apical transport of annexin XIIIb-associated Triton-insoluble membranes. *J. Cell Biol.* **2001**, *155*, 77−88.

(29) Burkhardt, J. K.; Echeverri, C. J.; Nilsson, T.; Vallee, R. B. Overexpression of the dynamitin (p50) subunit of the dynactin complex disrupts dynein-dependent maintenance of membrane organelle distribution. *J. Cell Biol.* **1997**, *139*, 469−484.

(30) Yamada, S.; Wirtz, D.; Kuo, S. C. Mechanics of living cells measured by laser tracking microrheology. *Biophys. J.* **2000**, *78*, 1736−1747.

(31) Burgess, S. A.; Walker, M. L.; Thirumurugan, K.; Trinick, J.; Knight, P. J. Use of negative stain and single-particle image processing to explore dynamic properties of flexible macromolecules. *J. Struct. Biol.* **2004**, *147*, 247−258.

(32) Burgess, S. A.; Knight, P. J. Is the dynein motor a winch? *Curr. Opin. Struct. Biol.* **2004**, *14*, 138−146.

(33) Burgess, S. A.; Walker, M. L.; Sakakibara, H.; Oiwa, K.; Knight, P. J. The structure of dynein-c by negative stain electron microscopy. *J. Struct. Biol.* **2004**, *146*, 205−216.

(34) King, S. M. AAA domains and organization of the dynein motor unit. *J. Cell Sci.* **2000**, *113*(Pt 14), 2521−2526.

(35) Hackney, D. D. The kinetic cycles of myosin, kinesin, and dynein. *Annu. Rev. Physiol.* **1996**, *58*, 731−750.